Equation of state and Raman-active E_{2g} lattice phonon in phases I, II, and III of solid hydrogen and deuterium

Yu. A. Freiman,[1,*] Alexei Grechnev,[1] S. M. Tretyak,[1] Alexander F. Goncharov,[2] and Russell J. Hemley[2]

[1] *B.Verkin Institute for Low Temperature Physics and Engineering of the National Academy of Sciences of Ukraine, 47 Lenin avenue, Kharkov, 61103, Ukraine*

[2] *Geophysical Laboratory, Carnegie Institution of Washington, 5251 Broad Branch Road NW, Washington, DC 20015, USA*

(Dated: February 24, 2013)

We present results of lattice dynamics calculations of the $P-V$ equation of state and the pressure dependence of the Raman-active E_{2g} lattice phonon for $p-H_2$ and $o-D_2$ in a wide pressure range up to ∼2 Mbar using our recently developed semi-empirical many-body potential, and density-functional theory. Comparison with existing body of experimental and theoretical results showed that the employed many-body potential is a reliable basis for high-precision calculations for phases I, II, and III of solid hydrogens.

PACS numbers: 64.30.Jk, 67.80.F-, 78.30.Am

An accurate determination of the equation of state (EOS) of solid hydrogens has been an important research objective for decades. Systematic high-pressure studies were started in the seventies of the last century[1–3] (see reviews[4–6] and references therein). At present these x-ray and neutron studies span the pressure range up to ∼2 Mbar[7–15] and temperature range up to 1000 K. The highest compression reached in the EOS experiments is 10.4 for solid H_2[15] (7.6 for solid D_2[14]), essentially higher than that for solid helium (8.4)[16]. The EOS data provide a fundamental basis for examining intermolecular interactions, and for testing *ab initio* theories. A number of model intermolecular potentials[17,18] have been proposed based on the experimental EOS data. Another experimental technique which complements x-ray and neutron diffraction by providing direct information on intermolecular interactions and vibrational dynamics is Raman scattering. The hcp structure has a Raman-active optical mode (E_{2g} symmetry) in the phonon spectrum which corresponds to the out-of-phase shear motions in the two orthogonal directions in the *ab* plane. The frequency range of this Raman mode is extremely large, from 36 cm^{-1} at zero pressure[19–27] to 1100 cm^{-1} at 250 GPa. The Raman spectrum of solid molecular deuterium has been measured up to ∼200 GPa[19–23,28,29]. These measurements show that hcp-based structures are stable in this pressure range. The calculations of the E_{2g} Raman frequency $\nu(P)$ using various empirical potentials[5,22,23] show that the result is highly sensitive to details of the potential used. Therefore, comparing the calculated and experimental $\nu(P)$ is a hard test for any empirical potential (or for any other theoretical method, e.g. *ab initio* calculations). It is essential that these properties are sensitive to different characteristics of the intermolecular potential: while EOS is sensitive to the potential well depth, the Raman scattering experiment probes the second derivative of the potential at the minimum. In our recent paper[30] we have proposed new semi-empirical isotropic potentials for H_2 and D_2. Unlike the previous potentials[12,17,18,31] they include not only pair forces, but triple forces as well. The goal of the present paper is to perform detailed calculations of the EOS and pressure dependence of Raman frequencies for H_2 and D_2 using our new potentials and to compare the results to available experimental data and theoretical results for a wide pressure range which spans the phases I, II, and III of solid p-H_2 and o-D_2.

As mentioned above, our potential includes pair (U_p) and triple ($U_{\rm tr}$) intermolecular forces ($U_{\rm tot} = U_p + U_{\rm tr}$). This potential was designed in a manner similar to the potential for solid helium[32,33]. It has the form of a sum of the pair Silvera-Goldman (SG) potential[17] (discarding the R^{-9} term) and three-body terms which include the long-range Axilrod-Teller dispersive interaction and a short-range three-body exchange interaction. The latter was used in a Slater-Kirkwood form[32,33]. Our potential also

includes the translational-rotational interaction however we have found that its contributions both to EOS and Raman frequencies are negligible. An explicit form and parameters of the employed potential are given in Ref.[30]. We restrict ourselves to $T = 0$ K, with the zero-point energy taken into account using the Einstein approximation. A small pressure range ($\sim$ 0.5 GPa) where quantum-crystal effects play a decisive role was excluded from consideration.

The decomposition of the total energy into contributions from the pair forces (E_p), triple forces (E_{tr}), and the zero-point energy (E_{zp}) is presented in Fig. 1. The inset of Fig. 1 shows the respective decomposition of EOS. As can be seen, the interplay between these three contributions is rather complicated and different for different regions of the molar volume. At relatively small compressions $V_0/V < 2$, the ground-state energy (and consequently the EOS) is dominated by the zero-point energy E_{zp}. The zero-point contribution decreases with rising compression, but it remains significant up to the highest pressures reached in EOS experiments. At the ten-fold compression the relative contribution E_{zp}/E_{gs} remains as high as 20%. It is interesting to note that for the eight-fold compression E_{zp}/E_{gs} coincides with that for solid ^{4}He, but for helium it increases with decreasing compression more steeply and already at three-fold compression the zero-point contribution dominates in the ground-state energy[16]. The three-body attraction becomes appreciable at the compressions higher than two-fold which corresponds to pressures about 2 GPa. The relative contribution of the tree-body forces $|E_{tr}|/E_p$ monotonically increases with pressure and for the eight-fold compression it reaches 0.5.

There has been many attempts to propose effective pair potentials which would have the same softening effect as attractive many-body forces[12,18,31]. To account for these effects Hemley *et al* modified the SG potential[17] with a short-range correcting term[12,31]. This Hemley-Silvera-Goldman effective potential was shown to fit static compression data up to 40 GPa. The $P(V)$ calculated with this effective pair potentials for higher pressures[14] increases far more

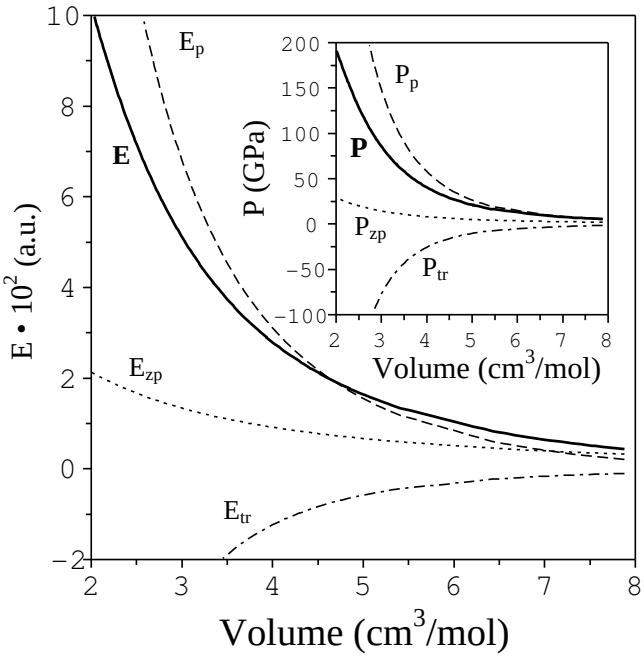

FIG. 1: Contributions of the pair E_p and triple E_{tr} forces, and zero-point energy E_{zp} to the total ground-state energy E_{gs} for solid p-H_2. The inset shows the respective contributions to EOS.

rapidly than in experiment.

The calculated equations of state $P(V)$ for solid hydrogen and deuterium are shown in Fig. 2 in comparison with DFT-GGA calculations[35] and the experimental results from Refs.[3,5,7,8,10,12,14,15,31]. As can be seen, the semi-empirical calculation with the proposed many-body potential is in an excellent agreement with experiment in the pressure range 1 - 140 GPa (phases I and II). These results can be compared favorably with recently published EOS calculations[34]. From 140 GPa onwards, the theoretical $P(V)$ curve lies slightly below the experimental one, and at the maximum pressure of 180 GPa (Phase III) the difference grows up to about 10%. The reason for this is the neglect of the higher order ($n > 3$) terms in the n-body expansion. The effect of the large-n terms increases with pressure, and at the metallization point the n-body expansion would converge extremely slowly. Methods based on the density functional theory (DFT) within local density approximation (LDA) and generalized gra-

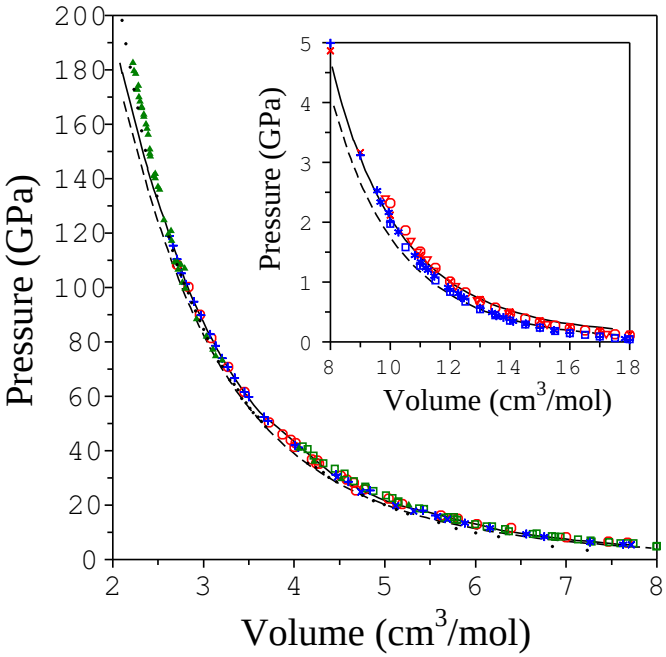

FIG. 2: (Color online) Calculated and experimental pressure-volume relations for solid H_2 and D_2. Semi-empirical calculations for many-body potential (this work): $p-H_2$ (solid line), $o-D_2$ (dashed line); DFT-GGA calculations $(\cdots)$[35]. Experiment (reduced to 0 K): (H_2: ▲[15], ○[14], □[5]); (D_2: +[14], ×[13], ∗[5]; the inset shows the small-pressure range. Experiment (reduced to 0 K): (H_2: ○[3], ×[10], ▽[7]); (D_2: □[3], +[10], ∗[8].

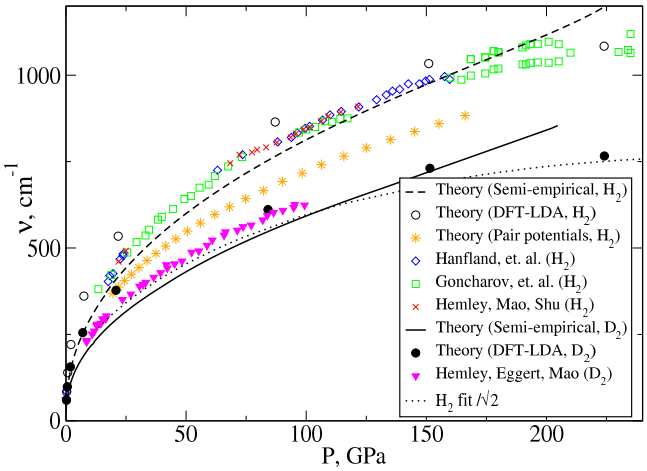

FIG. 3: (Color online) Calculated and experimental Raman frequencies as a function of pressure for solid hydrogen and deuterium. Semi-empirical calculations for many-body potential: this work. $p-H_2$ (dashed line), calculations for the SG potential ∗[5]; $o-D_2$ (solid line). DFT-LDA theory (this work): H_2 ○, D_2 ●. Experiment (H_2): ◇[24], ×[25]), □[26,27]; (D_2): ▽[29].

dient approximation (GGA) are somewhat of an opposite to the empirical potentials method. Indeed, the accuracy of the EOS from DFT-GGA[35] improves with the increase of pressure: in the pressure range 180-70 GPa the EOS from GGA practically coincides with the experimental one and for $P > 140$ GPa the agreement is better than for our empirical potentials, but at lower pressures the *ab initio* results progressively underestimate the pressure, and GGA gives a strongly underestimated equilibrium volume of about 8 cm^3/mol. The reason for this is twofold: first, GGA gives a poor description of the van der Waals forces, and second, DFT calculations ignore all quantum zero-point motions of nuclei, including the distinction between ortho- and para-species. We also compare theoretical and the experimental values for the isotopic shift $\Delta P(V) \equiv P_{D_2}(V) - P_{H_2}(V)$. In accordance with Ref.[14] we find that the empirical potentials strongly overestimate ΔP.

The comparison between theoretical and experimental pressure dependencies $\nu(P)$ of the E_{2g} optical phonon Raman-active mode is presented in Fig. 3. Since we could not find any DFT data of this mode in the literature, we have also calculated the E_{2g} Raman frequency of solid H_2 and D_2 in the $Pca2_1$ structure - one of the plausible candidates for the orientational structure of phases II and III - using DFT-LDA approximation. Our calculations were done using the Full-Potential Linear Muffin-Tin Orbital (FP-LMTO) code RSPt[36].

Comparing the theoretical results with the experiment we see that similarly to that we had for the EOS at pressures lower than ∼150 GPa the semi-empirical curves agree with experiment better than DFT calculations but at higher pressures the situation is reversed. The limiting pressures at which the semi-empirical approach still works are ∼175 GPa while LDA has a fine agreement with the experiment for H_2 and with frequencies obtained for D_2 with the help of harmonic ratio of $\sqrt{2}$ from 150 GPa up to the highest considered pressures ∼230 GPa. The frequencies calculated from the SG potential[17] deviate from experiment even for very low pressures. The same is true[5] for the effective HSG pair potential[12,31]. Thus we have shown that

while effective pair potentials work reasonably well for EOS up to 40 GPa, they fail for the dynamical properties like Raman spectrum, where the explicit inclusion of the 3-body forces is necessary.

In conclusion, we have calculated the EOS and the pressure dependence of the Raman-active E_{2g} mode using our recently proposed many-body potentials[30], and compared the results to the experiment and previous semi-empirical and DFT calculations. Also, DFT-LDA calculations of the E_{2g} Raman frequency were performed. For phases I and II ($P < 150$ GPa) the proposed many-body potentials give excellent agreement with the experiment, much better then any previous calculations. It proves that the new potentials are a reliable basis for high-precision calculations of structure and dynamics of H_2 and D_2 up to about 140 GPa. In particular, they provide a huge improvement over any effective two-body potentials, stressing the importance of including the 3-body forces. For the higher pressures (Phase III) the DFT approach is preferable.

* Electronic address: freiman@ilt.kharkov.ua

1 M. S. Anderson and C. A. Swenson, Phys. Rev. B **10** 5184 (1974). +

2 I. F. Silvera, A. Driessen, and J. A. de Waal, Phys. Lett. **68**, 207 (1978).

3 A. Driessen, J. A. de Waal, and I. F. Silvera, J. Low Temp. Phys. **34**, 255 (1979).

4 I. F. Silvera, Rev. Mod. Phys. **52**, 393 (1980).

5 H.-k. Mao and Russel J. Hemley, Rev. Mod. Phys. **66**, 671 (1994).

6 *Physics of Cryocrystals*, eds. V.G. Manzhelii and Yu.A. Freiman (AIP Press, New York, 1997).

7 S. N. Ishmaev, I. P. Sadikov, A. A. Chernyshov, B. A. Vindryaevskii, V. A. Sukhoparov, A. Telepnev, and G. V. Kobelev, Sov. Phys. JETP **57**, 228 (1983).

8 S. Ishmaev, I. Sadikov, A. Chernyshov, B. Vindryaevskii, V. Sukhoparov, A. Telepnev, G. Kobelev, and R. Sadikov, Sov. Phys. JETP **62**, 721 (1985).

9 R.M. Hazen, H. K. Mao, L. W. Finger, and R. J. Hemley, Phys. Rev. B **36** (1987) 3944.

10 van Straaten and Silvera, Phys. Rev. B **37** (1988) 1989.

11 H. K. Mao, A. P. Jephcoat, R. J. Hemley, L. W. Finger, C. S. Zha, R. M. Hazen, and D. E. Cox, Science **239** 1131 (1988).

12 R.J. Hemley, H.K. Mao, L.W. Finger, A.P. Jephcoat, R.M. Hazen, and C.S. Zha, Phys. Rev. B **42** (1990) 6458.

13 S. P. Besedin, I. N. Makarenko, S. M. Stishov, V. P. Glazkov, I. N. Goncharenko, A. V. Irodova, V. A. Somenkov, and S. Sh. Shil'shtein, High-Pressure research **4**, 447 (1990).

14 P. Loubeyre, R. LeToullec, D. Hausermann, M. Hanfland, R. J. Hemley, H. K. Mao, and L. W. Finger, Nature **383**, 702 (1996).

15 Y. Akahama, M. Nishimura, H. Kawamura, N. Hirao, Y. Ohishi, and K. Takemura, Phys. Rev. B **82**, 060101(R) (2010).

16 Yu. A. Freiman, S. M. Tretyak, A. Grechnev, A. F. Goncharov, J. S. Tse, D. Errandonea, H.-k. Mao, and R. J. Hemley, Phys. Rev. B **80**, 094112 (2009).

17 I. F. Silvera and V.V. Goldman, J. Chem. Phys. **69**, 4209, 1978.

18 M. Ross, F. H. Ree, and D. A. Young, J. Chem. Phys. **79**, 1487 (1983).

19 I. F. Silvera, W. N. Hardy, and J. P. McTague, Phys. Rev. B **5**, 1578 (1972).

20 M. Nielsen, Phys. Rev. B **7**, 1626 (1973).

21 P. J. Berkhout and I. F. Silvera, J. Low Temp. Phys. **36**, 231 (1979). 456 (1980).

22 R. J. Wijngaarden, V. V. Goldman, and I. F. Silvera, Phys. Rev. B **27**, 5084 (1983).

23 Ad Lagendijk, R. J. Wijngaarden, and I. F. Silvera, Phys. Rev. B **31**, 1352 (1984).

24 M. Hanfland, R. J. Hemley, H. K. Mao, High-Pressure Science and Technology -1993, edited by S. C. Schmidt et al. (AIP, New York, 1994), p. 877.

25 R. J. Hemley, H.-k. Mao, and J. F. Shu, Phys. Rev. Lett. **65**, 2670 (1990).

26 A. F. Goncharov, R. J. Hemley, H.-k. Mao, and J. F. Shu, Phys. Rev. Lett. **80**, 101 (1998).

27 A. F. Goncharov, E. Gregoryanz, R. J. Hemley, and H.-k. Mao, PNAS **98**, 14234 (2001)

28 R. J. Wijngaarden, and I. F. Silvera, Phys. Rev. Lett. **44**, 456 (1980).

29 R. J. Hemley, J. H. Eggert, and H.-k. Mao, Phys. Rev. B **48**, 5779 (1993).

30 Yu. A. Freiman, S. M. Tretyak, A. F. Goncharov, H.-k. Mao, and R. J. Hemley, Low Temp. Phys. 37, 1038 (2011) [Fizika Nizkikh Temperatur **37**, 1302 (2011)].

31 T. S. Duffy, W. Vos, C. S. Zha, R. J. Hemley, and H. K. Mao, Science **263**, 1590 (1994).

32 P. Loubeyre, Phys. Rev. Lett. **58**, 1857, 1987; Phys. Rev. B **37**, 5432 (1988).

33 Yu. A. Freiman,A. F. Goncharov, S. M. Tretyak, A. Grechnev, J. S. Tse, D. Errandonea, H.-k. Mao, and R. J. Hemley, Phys. Rev. B **78**, 014301 (2008).

34 L. Caillabet, S. Mazevet, and P. Loubeyre, Phys. Rev. B **83**, 094101 (2011).

35 L. J. Zhang, Y. L. Niu, T. Cui, Y. Li, Y. M. Ma, Z. He, and G. T. Zou, J. Phys.: Condens. Matter **19**, 425237 (2007).

36 J.M. Wills, M. Alouani, P. Andersson, A. Delin, O. Eriksson and O. Grechnyev, Full-Potential Electronic Structure Method: Energy and Force Calculations with Density Functional and Dynamical Mean Field Theory, Springer, Berlin, 2010.